conditions.

The boundary conditions are the normal fluid velocities specified at the elements' control positions. These, like the elements, are input to the programme in a clockwise direction, thus the first boundary conditions will indicate the inlet flow into the pipe, and the last ones will dictate the outlet flow. Intermediate ones will specify how much fluid is extracted or added through the wall of the pipe.

The first results from the finite element programme were obtained with uniform velocity profiles at inlet and outlet to the pipe. The suction or mass addition rates were also assumed constant down the pipe, and were evaluated remembering that continuity could not be violated. A typical example of boundary conditions used is given in Fig 4.5.

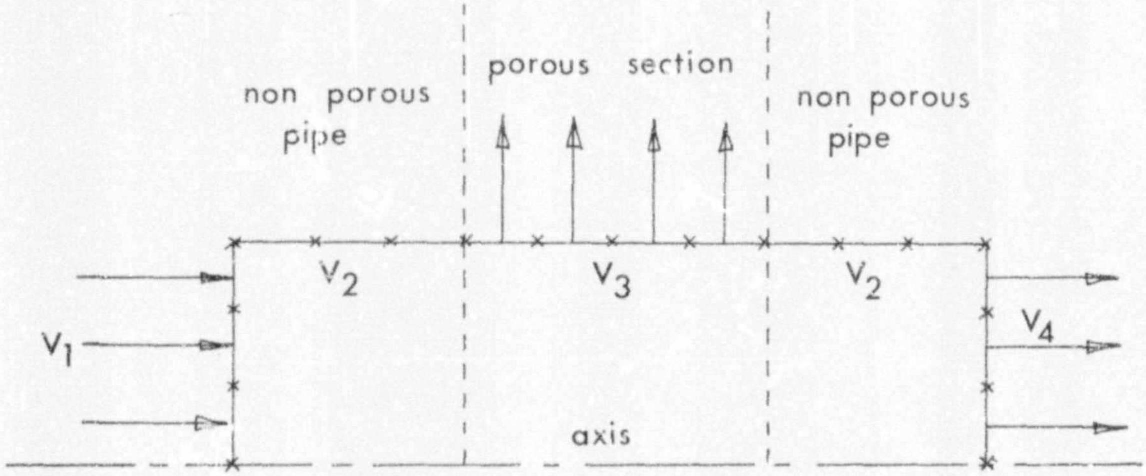

Fig 4.5 - Boundary Conditions specified at control positions

For the example given in Fig 4.5 the boundary conditions would be input into the programme as follows:

$+V_1$, $+V_1$, $+V_1$, 0, 0, 0, $-V_3$, $-V_3$, $-V_3$, $-V_3$, 0, 0, 0, $-V_4$, $-V_4$, $-V_4$.

The minus signs indicating fluid flowing out of the pipe. These are the values of F_j as described in section 3.3. Equation (3.5.2) is now solved for the unknown source strengths σ_i. In the computer programme this is done using a standard IBM subroutine for the inversion of the influence coefficient matrix A, this gives:

$$\sigma_i = (A^{-1}).(F_j) \quad . \quad . \quad . \quad . \quad . \quad . \quad . \quad . \qquad (4.7.1)$$

Because potential flow is assumed superposition of solutions is possible. One obvious solution of the problem is that the outlet and inlet flows are identical and there is no fluid transferred across the porous surface. This assumes that there is no friction at the pipe surface, but this is typical of a potential flow solution. In the other extreme it may be assumed that there is no total flow through the pipe in the axial direction but there is either mass addition or extraction through the porous wall. These two extremes are shown in Figs 4.6a, b and c.

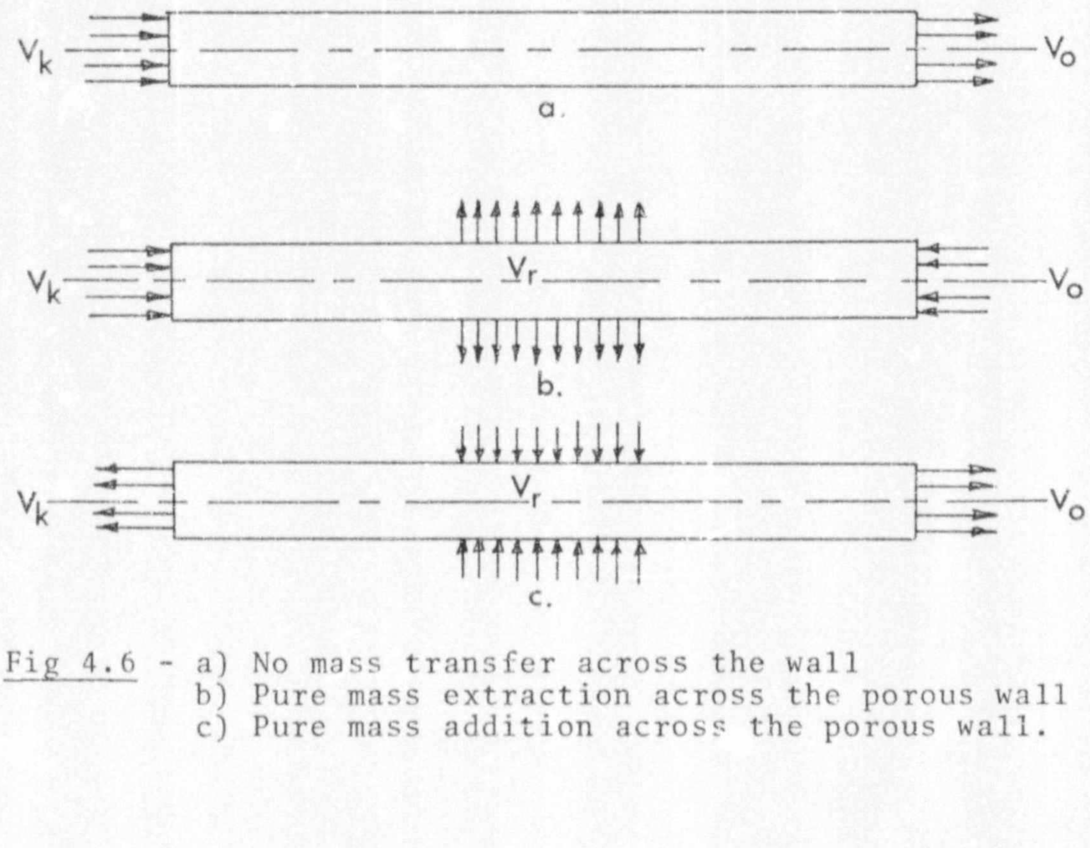

Fig 4.6 - a) No mass transfer across the wall
b) Pure mass extraction across the porous wall
c) Pure mass addition across the porous wall.

The superposition of a and b or a and c for different magnitudes of flow yields a whole range of different flow situations from large suction through zero transfer to large mass addition. Taking, for example, situation a) superimposed directly with situation b), the result will be given by the boundary conditions shown in Fig 4.7

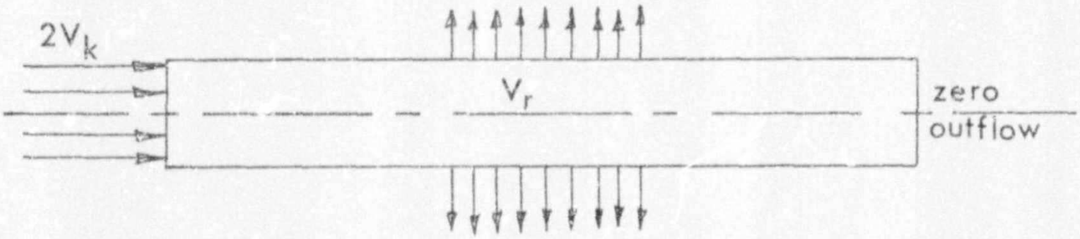

Fig 4.7 - Boundary conditions for situations shown in Figs 11a and b superimposed.

The resulting boundary conditions imply that all the fluid flowing down the pipe is extracted through the porous pipe and there is no outflow at the pipe exit.

It can be seen that the main problem is reduced to finding the solution to the boundary conditions given in Fig 11 b and c. These two flow fields are in fact identical, due to the potential flow nature of the problem.

Due to the discrete nature in which the boundary conditions are specified, it is possible to use any inlet and outlet velocity profiles, for example a parabolic profile may be used. The mass extraction or addition through the porous pipe may also take many forms, more detail is given concerning the choice of distribution in section 4.9.

4.8 Off Body Calculations

Once the source strengths distributed over each element have been calculated the whole flow field is evaluated.

Section 4.4 explains how the potential and velocities induced by an element at a point J may be calculated. J can be situated anywhere inside the pipe and the total effect, of all the elements, at J is given by the summation of the individual effect of each element. Thus the potential and velocity components at all points inside the pipe are calculated by using exactly the same numerical procedures as given in section 4.4. Special care is needed on the axis of the pipe, that is where $y_o = 0,0$, because the expression (4.4.4) which gives the radial velocity becomes singular here. There is no real difficulty, however, since the problem is axisymmetric there can be no radial velocity at $y = 0,0$, and so the value of y is examined in the programme and for $y_o = 0,0$, the radial velocity is assigned the value zero.

4.9 Mass transfer distributions through the porous pipe

Section 3.10 discussed the effects of axial pressure gradients on the mass transfer distributions along the porous pipe. It was decided to use Darcy's law in the form given by expression (3.10.2) (for the reasons explained in section (3.10)) to relate the radial velocity at the porous surface to the pressure drop across it. To begin the iterative procedure to calculate the actual transfer distribution along the porous pipe with a given inflow, (uniform velocity V_k, say,) and given outflow (uniform velocity V_o), it is necessary to assume an initial distribution. A constant transfer rate along the pipe is assumed and the total flow field is calculated as described previously.

In section 3.7 a coefficient of pressure was defined which related pressures in the pipe to the pressure at the inlet in order to be able to evaluate pressure recovery along the pipe. To enable comparisons with experimental work it is necessary to have information on the pressures existing inside the pipe in relation to atmospheric pressure. It was decided to test the programme assuming that the static pressure at the inlet was atmospheric pressure and required suctions were achieved by applying a back pressure at the exit to the pipe.

The computer programme calculates the coefficients of pressure at all control points on the porous surface, for the constant mass transfer rate. With these coefficients of pressure it is possible to modify the transfer rates according to equation (3.10.2), and rerun the programme. The only restriction on the mass transfer is that continuity is satisfied.

Using equations (3.7.1) and (3.10.2) gives:

$$V_r = k(p-p_a) = k(p-p_k) = \frac{kCp\rho V_k^2}{2} \quad . \; . \; . \; . \; . \quad (4.9.1)$$

Expression (4.9.1) may be used at every element's control position on the porous surface. If there are n elements defining the surface then there are n expressions of the form:

$$V_{r_1} = \frac{k\rho V_k^2 Cp_{k_1}}{2}$$

$$V_{r_2} = \frac{k\rho V_k^2 Cp_{k_2}}{2}$$

. . . . .

. . . . .

$$V_{r_n} = \frac{k\rho V_k^2 Cp_{k_n}}{2}$$

therefore:

$$\frac{V_{r_2}}{V_{r_1}} = \frac{Cp_{k_2}}{Cp_{k_1}}$$

. . . . (4.9.2)

. . . .

$$\frac{V_{r_n}}{V_{r_1}} = \frac{Cp_{k_n}}{Cp_{k_1}}$$

The total inflow to the pipe is $\pi R^2 V_k$. The total outflow (axially) along the pipe is $\pi R^2 V_o$.

The flow leaving through the porous surface must be given by:

$\pi R^2 (V_k - V_o)$

and this must remain constant.

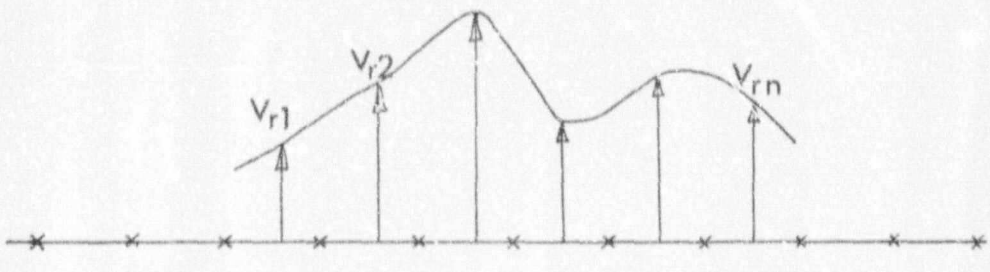

Fig 4.8 - Shows a velocity distribution along the porous surface.

The total integrated effect of a velocity distribution such as the one shown in Fig 4.8 is given by:

$$\text{total outflow} = 2\pi R.\Delta s(V_{r_1} + V_{r_2} + \ldots V_{r_n}) \quad . \quad . \quad . \quad . \quad (4.9.3)$$

where Δs is the length of an element, the integration uses a modified form of the trapezoidal rule.

Expression (4.9.3) may be rewritten as:

$$\text{total outflow} = 2\pi R\Delta s \; V_{r_1}(1+\frac{V_{r_2}}{V_{r_1}} + \ldots \frac{V_{r_n}}{V_{r_1}}) \quad . \quad . \quad . \quad . \quad (4.9.4)$$

which when using equations (4.9.2) becomes:

$$\text{total outflow} = 2\pi R\Delta s \; V_{r_1}(1+\frac{Cp_{k_2}}{Cp_{k_1}} + \ldots . \frac{Cp_{k_n}}{Cp_{k_1}})$$

but the total outflow must also equal

$$\pi R^2 (V_k - V_o)$$

and so an expression has been found for V_{r_1}:

$$V_{r_1} = \frac{R(V_k - V_o)}{2\Delta s(1+\frac{Cp_{k_2}}{Cp_{k_1}} + \ldots . \frac{Cp_{k_n}}{Cp_{k_1}})} \quad . \quad . \quad . \quad . \quad . \quad (4.9.5)$$

in terms of values known from the first computation.

Similarly from expressions (4.9.2), the other velocities may be calculated.

This new set of velocities describing the transfer rates across the porous wall are used as boundary conditions and the computer programme is re-run. A new set of pressures are calculated which in turn give a new set of transfer velocities. This iterative process is continued until equilibrium is reached, that is, when the pressures and velocities cease to change.

4.10 Calculation of Stream Lines

To be able to visualise the effects of various boundary conditions on the porous pipe flow problem it was found useful to visualise the flow field by plotting the stream lines.

As a datum the axis of the pipe is chosen to represent a stream line having the value of stream function $\psi = 1.0$. The computer programme calculates values of velocities in the radial and axial directions at points on, or inside, the pipe. Equations (3.8.1) are then used to calculate stream functions at these positions. Either expression may be used, one involves integration in the axial direction and the other in the radial direction. The integrations are performed using the trapezoidal rule. Integration in the radial direction is chosen as this is the most accurate since less integrations are required before the boundary is reached, thus reducing truncation errors due to the trapezoidal method.

A check was made on the accuracy of the method by comparing it with an integration performed in the axial direction. The results are indicated in the next section.

Once values of stream function have been evaluated, use is made of a standard contour plotting programme which plots lines of constant stream function (stream lines). Plots obtained for various boundary conditions are given in Chapter 6 a typical one is given in section 4.11.

The output from the computer programme also calculates the potential at positions on and inside the pipe. These are also plotted by the contour programme and the results appear in the next section.

4.11 Typical Results obtained from the Computer Programme

A full set of results obtained from the computer programme for various boundary conditions is given in the appendix. This section illustrates the format used in presenting the results and discusses important aspects in relation to the method of programming.

It was mentioned in section 4.7 that because superposition of flows was possible the main problem was reduced to the solution of the boundary conditions given in Fig 4.9.

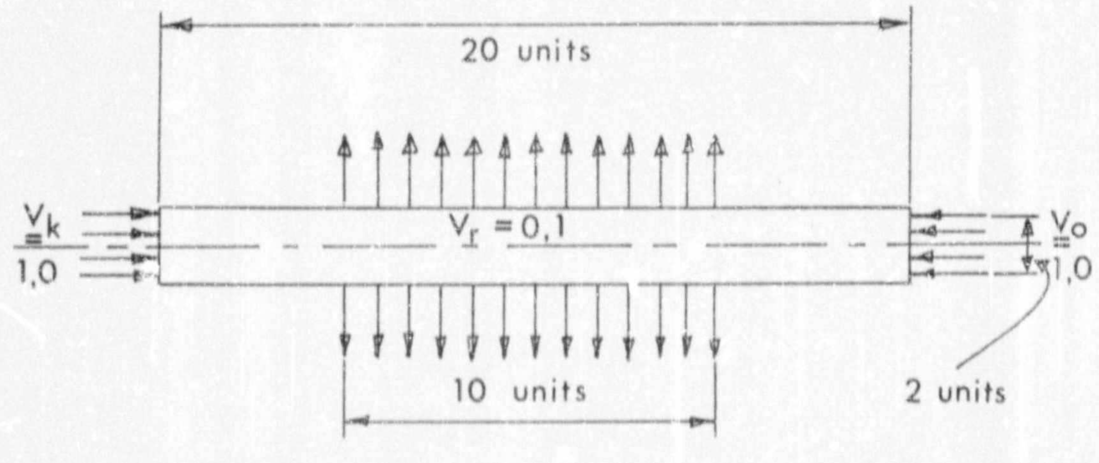

Fig 4.9 - Boundary conditions for the solution of the basic problem

Using the boundary conditions given in Fig 4.9 the pressure coefficient Cp, calculated by the programme plotted against axial distance along the pipe for various radial positions, is shown in Fig 4.11. The porous section of the pipe is labelled. It can be seen to be displaced slightly about the centre line, this is due to the way in which the elements were defined. The programme requires an even number of input points as use is then made of the symmetry of the problem thus omitting duplication of calculations. To enable a porous section ten units long the boundary conditions used were as shown in Fig 4.10.

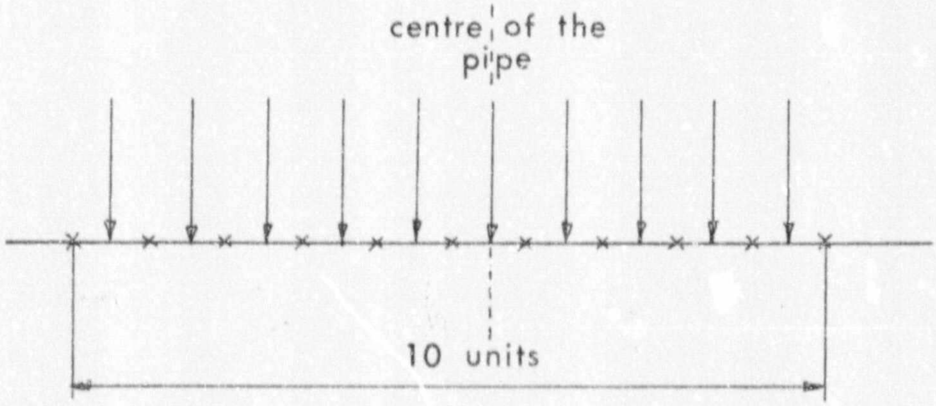

Fig 4.10 - Shows the displacement of the porous section to the left to enable a section 10 units long to be used.

This displacement about the centre line in no way effects the results as can be seen from graphs 4.11 and 4.12. From Fig 4.11 it is noticed that pressure gradients in the radial direction are almost negligible.

Figure 4.12 shows the stream lines calculated for the boundary conditions given in Fig 4.9. The stream lines in fig 4.12(a) were evaluated by integration in the radial direction and those in Fig 4.12(b) by integration in the axial direction. The two plots appear to be extremely similar, any differences are due to the errors introduced by the trapezoidal procedure used in the integration, which should be more pronounced in Fig 4.12(b).

Figure 4.13(a) and (b) illustrate lines of constant potential and lines of constant stream function for the boundary conditions given in Fig 4.9. The lines of constant potential are calculated directly from the potential flow method; the lines of constant stream function are calculated by integration of velocities in the radial direction.

As is expected, from potential flow theory, the lines in the two plots are orthogonal, which indicates that the method of calculating the stream functions is adequate.

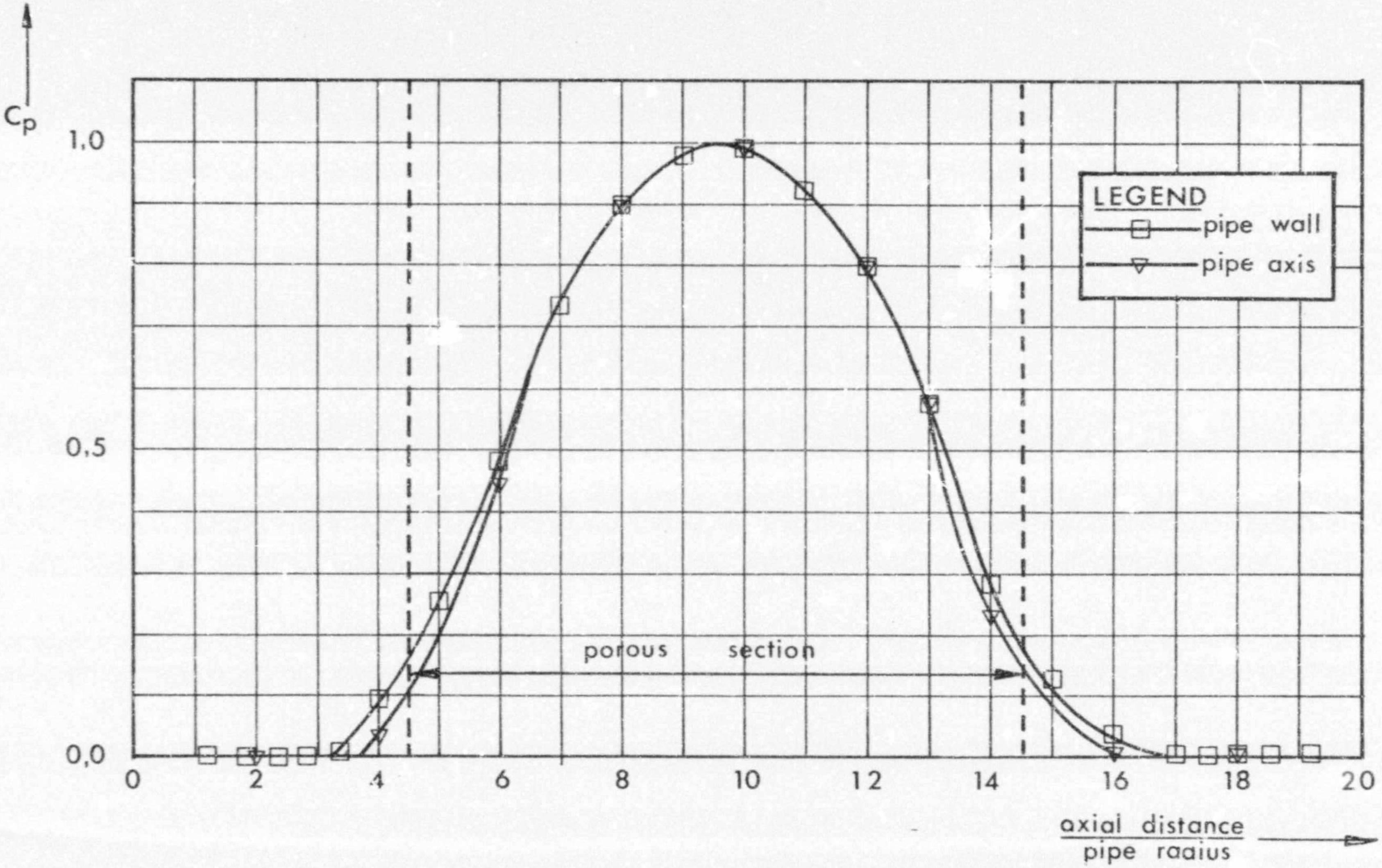

FIG 4.11 VARIATION OF Cp ALONG THE PIPE FOR THE BOUNDARY CONDITIONS GIVEN IN FIG 4.9

Fig 4.12 - The streamlines calculated for the boundary conditions of Fig 4.9

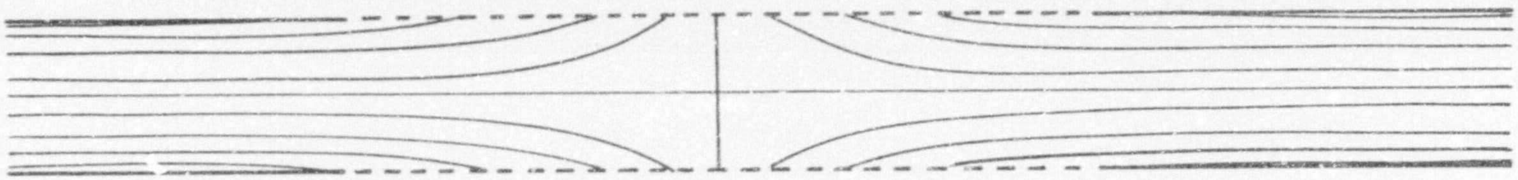

a) by integration in the radial direction

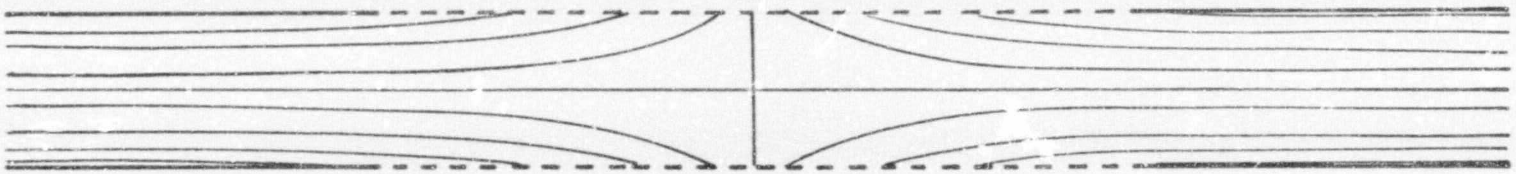

b) by integration in the a[illegible]l direction

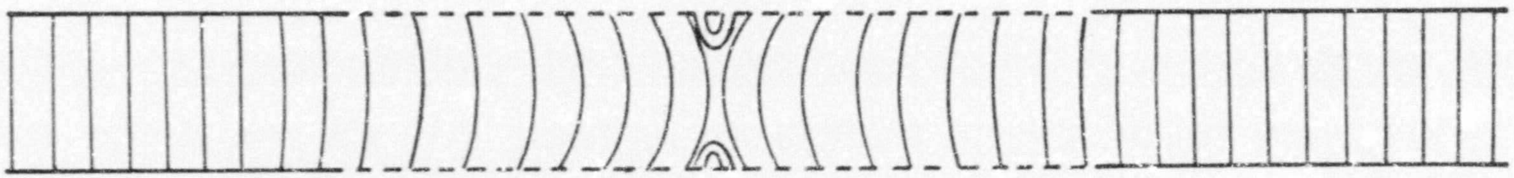

Fig 4.13 a) Lines of constant potential for the boundary conditions given in Fig 4.9

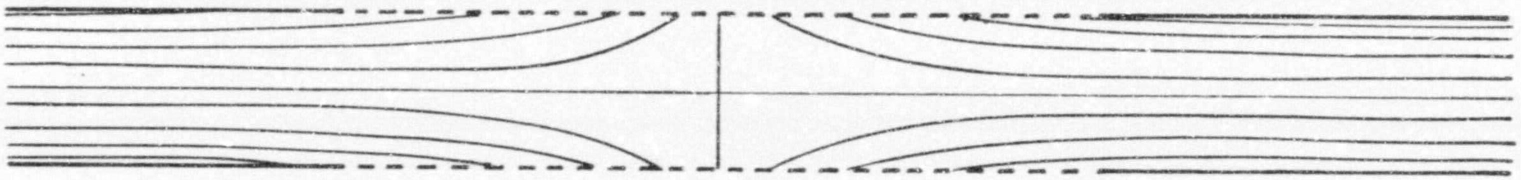

Fig 4.13 b) Lines of constant stream function for the boundary conditions given in Fig 4.9

CHAPTER 5

EXPERIMENTAL APPARATUS & PROCEDURE

5.1 Introduction

The purpose of the experimental work was twofold. Firstly it was desirable to have a wide range of results for comparison with the theories and experimental work described in Chapter 2. Secondly with sufficient experimental data a critical appreciation of the theory developed in Chapters 3 and 4 could be made.

It was essential that the experimental apparatus be as versatile as possible so that a range of data, for comparison with previous research in the field, could be collected. This involved the ability to have laminar or turbulent flow in the porous pipe and a whole range of suction and blowing velocities through the porous surface.

This chapter discusses the design of the experimental apparatus and the measuring techniques employed. A detailed description is given of the experimental procedure and any difficulties encountered during the experimentation are mentioned.

5.2 The Air Supply

To enable a wide range of data to be collected it was necessary to have an air supply which could deliver a variety of volume flow rates. The obvious choice was a centrifugal fan. When the design of the working section was commenced, it was found that to be able to obtain a large range of suction velocities, a higher pressure, than was available from a centrifugal fan was required. (The design of the working section is described in section 5.4) The compressed air supply available in the laboratory gave a sufficiently high pressure but was unable to deliver air at the required volume flow rates. The air would have needed to be filtered before it was introduced into the porous specimens as it contained moisture and grease droplets.

The final choice of air supply was a Roots type blower made by Howden Godfrey Ltd, driven by a variable speed belt type transmission. This was a positive displacement blower which could deliver oil-free air up to a pressure of one atmosphere. Its maximum available air flow rate at sea level was 1 020,0 m^3/hr at 0,825 bar gauge pressure. The delivery end was fitted with a pressure relief valve of the spring loaded plate type. The speed of the blower, and hence air flow rate, could be varied by changing the setting of the belt transmission. On the inlet side to the blower the air was cleaned through a foam filter thus eliminating particles down to five microns. Also on the inlet side was an orifice plate together with pressure tappings and a thermocouple to enable direct comparisons between air flow rates at the blower and those measured through the apparatus.

When in operation, especially under severe loading, the air would leave the blower at temperatures ranging from 60 ^{0}C to 90 ^{0}C. It was therefore necessary to cool the air before it reached the working section of the apparatus.

The blower was situated on the roof of the laboratory where it was permanently installed. Air was delivered to the apparatus through a 101,6 mm diameter (four inch nominal diameter) pipe which passed along the length of the roof (through approximately thirty meters of piping), and down into the laboratory. It was decided, for simplicity, to cool the air by using an annular cooler positioned as close as possible to the blower where the temperatures of the air were highest. Due to the greater heat transfer where the air was hottest a shorter cooler could be used than if it was positioned closer to the apparatus. Water was used as the cooling fluid and the detailed design of the cooler is given in the appendix.

After leaving the cooler the air expanded into smaller diameter piping in the laboratory thus undergoing a further temperature decrease. A schematic diagram of the air supply is given in Fig 5.1.

5.3 Flow Regulation and Measurement

Fig 5.2 shows the general layout of the testing facility. A more detailed account of the working section is given in section 5.4.

Air entered the laboratory from the blower via 101,6 mm diameter (four inch nominal diameter) piping. The blower and apparatus were protected by a by-pass valve which was always in the fully open position when the blower was started, thus allowing a minimum amount of air to pass through the apparatus and the bulk of it to be discharged through the by-pass into the atmosphere. As the by-pass valve was closed so the air flow through the apparatus increased. An orifice plate of 80 mm diameter (orifice plate number one) conforming to British Standard code

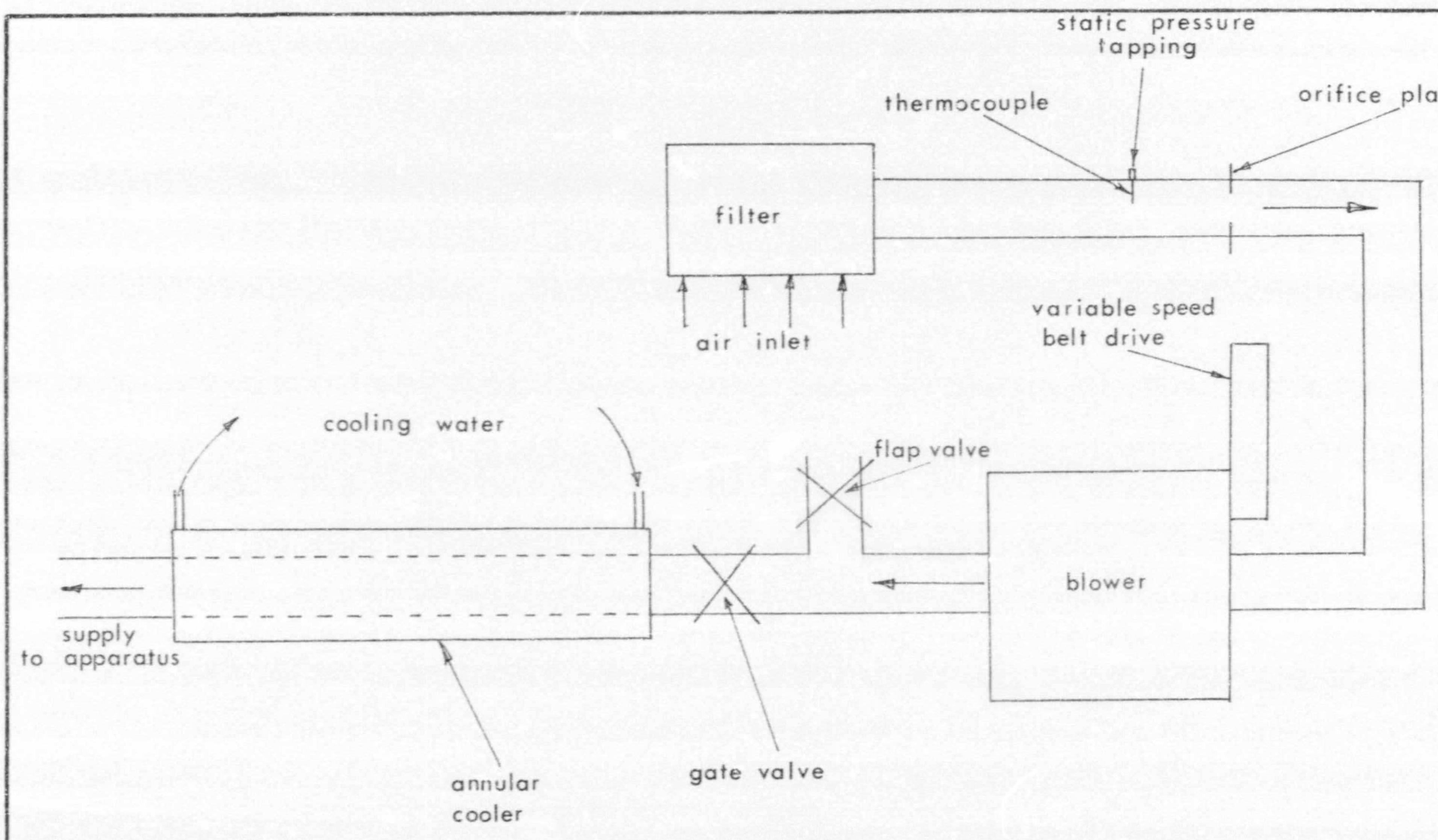

FIG 5.1 SCHEMATIC OF THE AIR SUPPLY

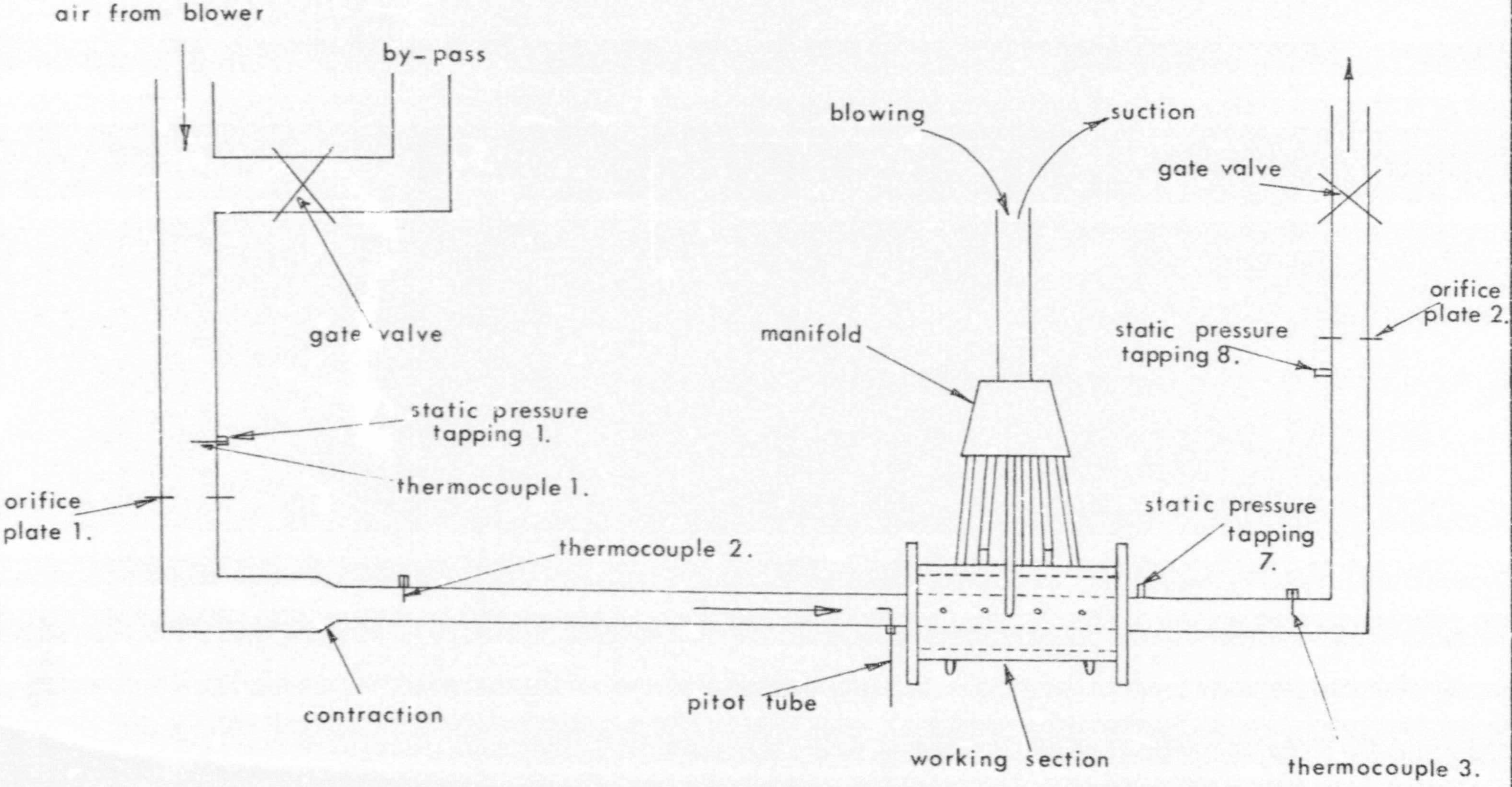

FIG 5.2 . SCHEMATIC OF THE TEST RIG

B S 1042 was used to measure the volume flow rate through the apparatus. It was installed in the network according to the standards. A pressure tapping at the high pressure side of the orifice plate measured the static pressure by means of a mercury U-tube manometer with one end open to the atmosphere (static pressure tapping number one). The air temperature at the high pressure side was measured by means of a copper constantan thermocouple. The cold junction was kept at 0 ^{0}C in a vacuum flask of well stirred melting ice, the voltage in milli-volts was measured using a Cambridge potentiometer. The calibration charts for the thermocouples used in the experiments are given in the appendix. The pressure difference across the orifice plate was measured with a water filled U-tube manometer.

The working section of the apparatus was designed for three different diameter porous pipe specimens. They were of 25,4; 44,45 and 63,5 mm internal diameters. After orifice plate 1 it was necessary to have a contraction in the pipe to enable the various size specimens to be accommodated. Tests were only conducted on specimens of 63,5 mm internal diameters due to the time available, however, the apparatus does not require any further modifications to allow for tests on the other sizes.

After the contraction it was necessary for there tc be a sufficient length of straight piping before the working section, to allow for the flow to settle down, and any swirl induced by the orifice plate and the bend to be eliminated. The length of pipe according to B S 1042 was approximately 2,5 meters. Introduced into this pipe was another thermocouple which allowed temperature measurements to be made after the contraction and before the working section, for reasons that will be explained in section 5.5.

Before the air entered the working section of the test facility a traverse of the flow was made with a miniature pitot-static tube of 0,65 mm internal diameter. The tube was connected by means of rubber tubing to a water U-tube manometer, thus enabling a measurement of the dynamic pressure inside the pipe to be made. Also at this station measurements were made of the static pressure (static pressure tapping number two) by removing the rubber tubing from one side of the pitot tube. Measurements were taken at positions 25 mm apart across the cross-section of the pipe. The traversing mechanism and pitot tube are illustrated in Fig 5.3.

After the working section the static pressure of the air was measured at pressure tapping number seven (see Fig 5.2) attached to a mercury U-tube manometer. Further down stream another thermocouple measured air temperature (thermocouple number three). Prior to the second orifice plate the static pressure was again monitored on a mercury manometer. Orifice plate 2 had an orifice diameter of 41,3 mm in a pipe of 50,8 mm internal diameter (two inch nominal diameter). The pressure difference across the plate was measured with corner pressure tappings and a mercury manometer.

Following orifice plate 2 the air exhausted to atmosphere via a gate valve. By controling this valve the amount of air flowing through the orifice plate to the atmosphere could be regulated. As the valve was closed so more air was forced to flow through the walls of the porous pipe, through the manifold and into the atmosphere. In this way for a given volume flow rate of air through the apparatus, regulated by the by-pass gate valve, suction through the walls of the porous pipe could be controlled by varying the back pressure on the working section by means of the outlet valve.

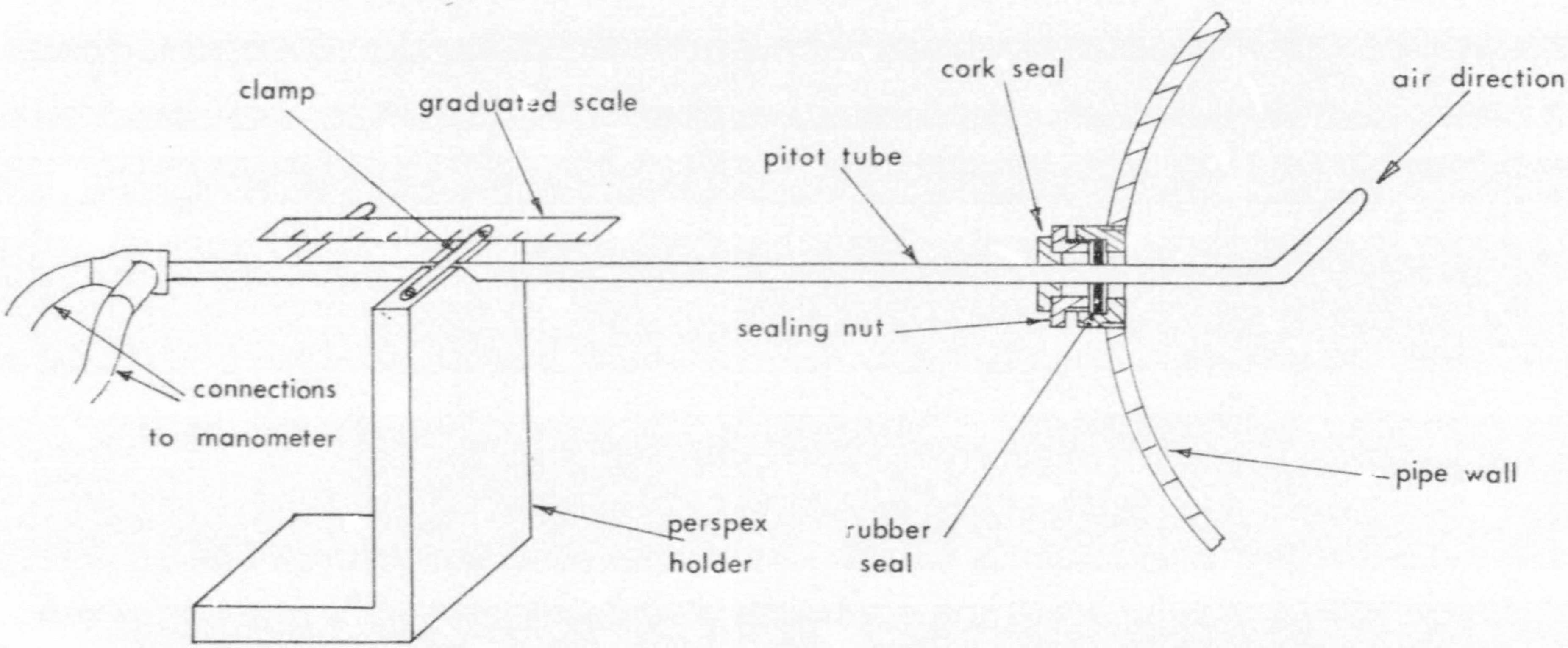

FIG 5.3 THE PITOT TUBE TRAVERSING MECHANISM

By attaching the outlet of the manifold to the compressed air supply, in the laboratory, air could also be introduced into the porous pipe, these blowing tests were not conducted due to the time available.

5.4 The Working Section

The porous specimen that was tested was made of sintered bronze manufactured by Sintered Products Ltd, of Nottingham, England. It had an internal diameter of 63,5 mm, an external diameter of 69,85 mm and was approximately 25,5 mm long. The manufacturers produce the sintered bronze in five different grades. They are A, B, C, D and E according to the porosity. Grade A is least porous and grade E is highly porous. The grade of material used for the tests was D, thus indicating a moderate to high porosity. The manufacturers claim that this grade allows the passage of particles less than 25 microns.

The test specimen was held in place by mild steel flanges (See Fig 5.4). Surrounding the specimen was another porous pipe of 111,1 mm internal diameter and the same length as the test section, this was manufactured from Porosint grade C sintered bronze (maximum particle diameter able to pass is 12,5 microns). This larger pipe was used as a control Initially the working section was designed for both blowing and suction tests, and the larger porous pipe was situated so that, during blowing tests, the inner test pipe would experience uniform blowing over its surface. In the suction tests it also served a similar purpose as the air that was expelled through the walls of the inner pipe was then forced to pass through the outer pipe before it flowed into the rubber tubing connecting the working section

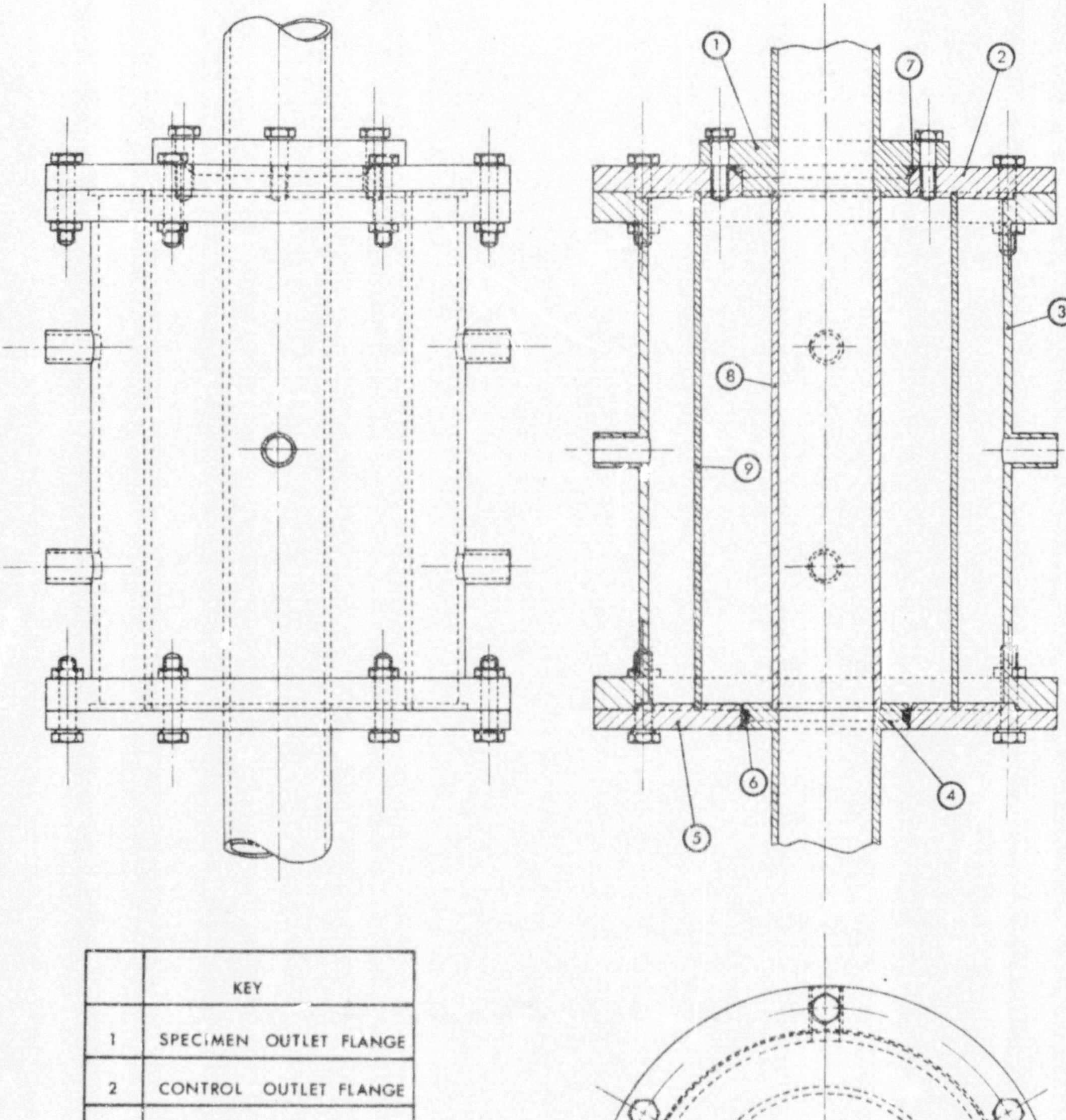

	KEY
1	SPECIMEN OUTLET FLANGE
2	CONTROL OUTLET FLANGE
3	CONTROL CYLINDER
4	SPECIMEN INLET FLANGE
5	CONTROL INLET FLANGE
6	GACO 'O' RING
7	GACO 'O' RING
8	POROUS SPECIMEN
9	POROUS CONTROL

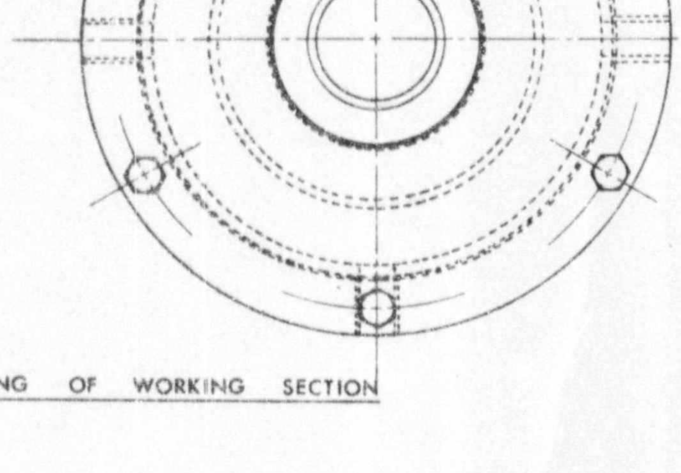

FIG. 5.4. ASSEMBLY DRAWING OF WORKING SECTION

to the manifold. This ensured that the inner pipe was completely isolated from any adverse effects the manifold may have had, such as applying irregular suction over the pipe surface.

Surrounding both porous pipes was a steel pipe of 168 mm internal diameter which had six outlets distributed around its surface. These delivered air, via rubber tubing, to the manifold as illustrated in Fig 5.2 and shown in more detail in Fig 5.4. It was possible to prevent flow from leaving the working section through the walls of the porous pipes by tightening clips around the rubber tubing. This enabled tests to be performed with no mass transfer to or from the system.

The working section was sealed using Gaco - 'O' rings, these are indicated in the assembly drawing Fig 5.4. The apparatus was designed so that a variety of different specimens could be tested inside the basic working section by simply removing the inlet and outlet pipes and flanges and replacing them with different sizes. Detailed drawings and dimensions of the components in the working section are given in the appendix.

The working section was rigidly supported on a handy angle framework as shown in Fig 5.6.

Measurements of velocities in the axial and radial directions within the porous specimen were made with hot-wire probes. The probes were introduced into the working section through four aluminium guide tubes, of six millimeter internal diameters, which penetrated the three layers of piping. They are illustrated in Fig 5.5. They were also used as static pressure tappings.

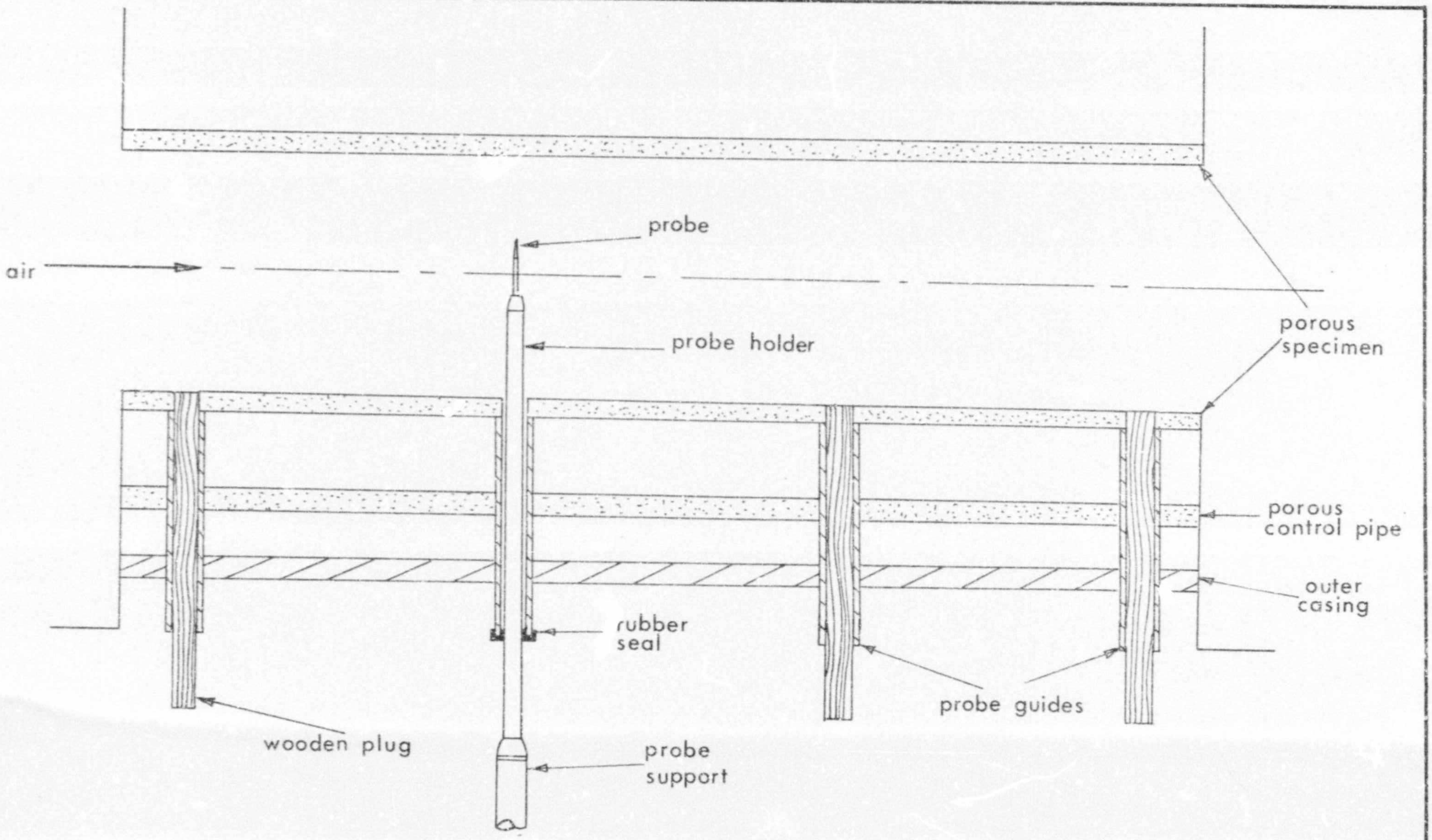

FIG 5.5 THE HOT-WIRE PROBE TRAVERSING POSITIONS